Solute Diffusion in Polymers. 1. The Use of Capillary Column Inverse Gas Chromatography

Craig A. Pawlisch,† A. Macris, and Robert L. Laurence*

Department of Chemical Engineering, University of Massachusetts, Amherst, Massachusetts 01003. *Received June 30, 1986*

ABSTRACT: A technique using inverse gas chromatography (IGC) for accurately measuring polymer–solute diffusion coefficients has been developed. The technique is ideal for studying interactions of volatile materials with molten or rubbery polymers, at conditions approaching infinite dilution of the volatile component. Previous efforts used to measure diffusivity via a chromatographic technique have used packed columns, with polymer supported as a thin, irregular coating on the packing. The irregularity of the coating severely limits measurement accuracy. This difficulty is overcome by using a capillary column with a relatively thick, uniform coating, which admits more realistic mathematical models for parameter estimation. The polymer, the stationary phase in the experiment, is deposited as a uniform annular coating on the inside of a glass capillary column. A solute is injected into an inert carrier gas flowing through the column. The elution characteristics of the sample (residence time and shape of the elution curve) are used to determine the solute activity and diffusivity in the stationary phase. The validity of the technique was demonstrated by measuring the diffusivity and activity of benzene, toluene, and ethylbenzene in polystyrene between 110 and 140 °C. The thermodynamic properties obtained were in good agreement with existing packed-column IGC and vapor sorption data. The diffusion coefficients obtained were consistent with existing vapor sorption measurements.

Introduction

The solubility and diffusivity of the low molecular weight components of a polymer solution are fundamental physical properties frequently required for the design of many polymer synthesis and fabrication operations. Conventional methods for measuring these properties rely on sorption and bulk equilibration. These are difficult to apply to polymer–solute systems when the solute is present in vanishingly small amounts. The time for sorption may be large because the diffusion coefficient may be small. Accuracy suffers because the amount of solute is small. As a consequence, there is a dearth of published data regarding the solubility and diffusivity of common solvents in commercially important polymers.

In recent years, gas chromatography has become well established as an alternative for studying the interaction of polymers with volatile solutes.[1-4] In a typical application, the polymer is used as the stationary phase in a chromatographic column. The solute or probe is vaporized and injected into a carrier gas flowing through the column. As the probe is swept through the column, it can interact with the polymer via adsorption or absorption. The retention time of the probe and the shape of the elution profile (i.e., chromatographic peak) will reflect the strength and nature of the interactions that occur between the polymer and the solute and can be used to study those interactions. Such an experiment is sometimes referred to as inverse gas chromatography (IGC), to differentiate it from the more common analytical applications of gas chromatography.

To date, IGC has been used primarily for the measurement of solution thermodynamic parameters. When an IGC experiment is carried out at temperatures significantly higher than the glass transition temperature of the polymeric stationary phase, the retention time will be determined by the solubility of that component in the polymer. Consequently, measurements of retention time can be used to calculate such useful parameters as Henry's law constant, the activity coefficient, and various solution model interaction parameters.

In comparison with bulk equilibration methods (gravimetric sorption/desorption) for thermodynamic measurements, IGC offers several advantages. The foremost among these is speed: a single IGC experiment can be completed in minutes; a vapor sorption experiment may require hours or days to complete. The method is ideal for obtaining infinite dilution properties because very low solute concentrations can be measured with standard detector systems. In addition, changes in the solute and temperature can be readily made in a chromatographic experiment. These features enable determination of the interactions of a large number of solutes with a given polymer in a relatively short period of time. Several studies have established the consistency of thermodynamic data obtained by IGC with data obtained by more conventional techniques.[5-8]

In principle, IGC experiments can also be used to obtain information about the diffusion of the solute in the polymer phase. It has long been recognized that mass-transport limitations in the stationary phase result in significant spreading and distortion of a chromatographic peak. A number of researchers have attempted to exploit this phenomenon as a means of measuring the diffusion coefficient of the solvent in the stationary phase.[7,9-13] In all of these studies, packed-column chromatography was used and diffusion coefficient estimates were extracted from the elution curve data using the van Deemter equation. None of these efforts has provided a convincing demonstration that the method can be used to obtain meaningful information; difficulties inherent in the use of a packed column make it nearly impossible to relate the measured elution curve to the diffusion coefficient. The major limitation is the irregular distribution of polymer with the column, which prohibits the application of realistic models for stationary phase transport processes.

In this paper, we present a significant improvement in the IGC method for the measurement of diffusivities. The technique is based on the use of capillary chromatographic columns with highly uniform coatings of polymer, which admits the use of more realistic models for parameter estimation. In what follows, we review earlier methods for estimating diffusivity from IGC data, present the mathematical model used to describe capillary column IGC, describe the experiment, and present data on several

†Current address: Research Laboratories, Union Camp Corp., Princeton, NJ 08540.

0024-9297/87/2220-1564$01.50/0

well-characterized polymer–solute systems as a basis for comparison with other methods.

Background

Gas chromatography (or GC) is based on the characteristic equilibrium partitioning of a solute between a mobile phase and a stationary phase, arising from bulk absorption (or surface adsorption) of the solute by the stationary phase. As a solute sample passes through a chromatographic column, a fraction of that sample will always reside in the stationary phase. As a consequence, the mean residence time of the sample will be greater than the mean residence time of a gas-phase component that does not absorb in the stationary phase.

The simplest theory of gas chromatography (e.g., ideal chromatography) neglects the details of the mass transport within each phase and assumes that the partitioning of the solute between the stationary and mobile phases reaches an equilibrium state instantaneously. Such a description of the chromatographic process does not take into account the axial dispersion of the solute and, hence, implies that the elution profile is identical with the inlet profile. According to the simplest theory, partitioning serves only to reduce the mean axial velocity of the solute. In reality, mass-transport processes are never completely negligible; partitioning of the solute always proceeds at a finite rate. The existence of transport resistances, which hinder the transport of solute between the phases, inevitably produces axial spreading and distortion of the solute pulse as it travels through the column. Additional contributions to the dispersion of the pulse are expected from a variety of transport processes.

Originally, researchers were interested in this phenomenon as it related to separation efficiency in analytical applications. It was also recognized that, at least in principle, measurements of peak spreading and distortion could be used to obtain estimates of the diffusion coefficient of the solute in the stationary phase. The major problem in implementing such an experiment is that, in addition to stationary-phase transport, many other processes can influence peak shape. Some of the more significant include axial gas-phase dispersion, channeling of the carrier gas, back-mixing in the injector and detector, nonuniform injection of sample, gas-phase mass-transfer resistance, surface adsorption effects, and nonlinearity of the absorption isotherm. These other factors must either be suppressed in the experiment or accounted for in the model used to analyze the data.

Virtually, all reported applications of IGC to the measurement of diffusion coefficents have used packed chromatographic columns, in which the stationary phase is supported on a granular substrate. Equations similar to that developed by van Deemter et al.[14] are used to calculate the stationary-phase diffusion coefficient from the spreading of the elution profile. The equation developed by van Deemter is commonly written as

$$H = A + B/V + CV \tag{1}$$

where H is the height equivalent to a theoretical plate (HETP) and V is the mean velocity of the carrier gas. The constants A, B, and C represent the contributions of eddy diffusion, gas-phase molecular diffusion, and stationary-phase mass-transfer resistances toward broadening of the peak. The equation is only valid for describing the elution of symmetric peaks, which requires that mass-transfer resistances be small but not negligible. From plate theory, it can be shown that for a column producing Gaussian-shaped peaks the HETP is related to the peak width or variance by the following:[2]

$$H = L\{\sigma_t^2/t_r^2\} = L/t_r^2\{W_{1/2}/2.335\}^2 \tag{2}$$

where L is the column length, σ_t^2 is the variance of the peak, t_r is the retention time of the peak, and $W_{1/2}$ is the width of the peak at half-height.

For the case in which all mass-transfer resistance is due to diffusion in the stationary phase and the stationary phase is uniformly distributed on the surface of a uniform spherical packing, the constant C is related to the solute diffusivity by[14]

$$C = (8/\pi^2)(T/D_p)(K/\epsilon)[1 + (K/\epsilon)]^{-2} \tag{3}$$

where D_p is the diffusion coefficient in the stationary phase, τ is the film thickness, K is the partition coefficient, and ϵ is the ratio of the stationary-phase volume to the gas-phase volume.

These results may be used to determine diffusivity from experimental data as follows: Solute elution curves are obtained for a range of flow rates. From measurements of peak width, a plot of H vs. V is prepared. At sufficiently high flow rates, the second term on the right-hand side of eq 1 becomes negligible and the plot will be linear. From the measured slope, D_p will be calculated with eq 3. It is presumed in the analysis that diffusion in the stationary phase is Fickian and that the diffusion coefficient is concentration independent.

This technique is especially well suited to the study of very small diffusivities. When the solute diffusivity is low, diffusion within the stationary phase is the dominant process determining the shape of the elution profile, so that the contribution of other processes can be neglected more readily.

Conventionally, diffusion coefficients for solutes in molten polymers are determined by gravimetric sorption/desorption experiments. A sample of known weight and shape is placed on a sensitive balance and exposed to a constant concentration of solute. From the weight gain of the sample vs. time, a diffusion coefficient can be calculated. Crank and Park[15] and Crank[16] review the method in detail. Disadvantages of the technique include the relatively long time required for a single measurement, the difficulty of maintaining a constant, simple geometry for the molten sample, and the need to use solute concentrations large enough to produce measurable weight changes. These constraints limit the accuracy of measurements at conditions approaching infinite dilution of the solute and for systems where the diffusion coefficient is strongly concentration dependent. In contrast, a chromatographic technique is significantly faster, more convenient, and ideally suited to measurements approaching infinite dilution.

Despite these advantages and despite the widespread use of IGC for thermodynamic measurements, there have been relatively few applications to the study of polymer–solvent diffusion. The first reported use was by Gray and Guillet,[17] who studied the diffusion of benzene, decane, and dodecane in polyethylene and natural rubber. They were unable to prepare suitable columns with natural rubber but did obtain reasonable diffusion coefficients with polyethylene. Braun, Poos, and Guillet[9] measured diffusion coefficients for n-decane, tetralin, decalin, and two commercial plasticizers in polyethylene. Kong and Hawkes[10] and Millen and Hawkes[11] have studied the diffusion of n-chain alkanes in dimethylsilane polymers. Galin and Rupprecht[12] measured the diffusion coefficients of several organic solvents in polystyrene. Tait and Abushihada[7] used the method to study the diffusion of a number of organic solvents in poly(vinyl chloride), polystyrene, and poly(methyl methacrylate). Senich[13] mea-

sured the diffusion coefficient of octadecane in high-density polyethylene.

Motivation for This Work

The accuracy and reliability of IGC measurements is difficult to judge from the rather limited number of studies, primarily because of the dearth of reliable information with which to compare results. The method has been subject to criticism that has cast doubt on the potential accuracy. The most serious concerns are summarized below:

(1) The van Deemter analysis assumes a uniform distribution of polymer. In any real packed column, the distribution will not be uniform and will be difficult to characterize. The nature of the polymer distribution will have a major effect on peak broadening. Senich[13] has pointed out that for a given set of data, models based on uniform and highly nonuniform distributions will yield diffusion coefficients that differ by 3 orders of magnitude.

(2) Transport of solute between the mobile and stationary phase is described by an effective mass-transfer coefficient that contains the polymer-phase diffusion coefficient; the solute flux across the interface is assumed to be proportional to the difference between the mean value of the stationary-phase and the mobile-phase solute concentrations. When concentration gradients in the polymer phase are steep, such a model will underestimate solute flux and provide a poor description of the processes that determine peak shape. A more rigorous formulation would use the diffusion equation to describe transport in the polymer layer.

(3) The model assumes that gas-phase axial dispersion is correctly described by an effective dispersion coefficient that is independent of the gas velocity and treats instrumental broadening as a constant. Neither assumption is likely to be true, making it more diffult to measure the true contribution of polymer-phase diffusion to peak broadening. Because gas-phase dispersive processes are responsible for a significant fraction of the peak broadening that occurs in a packed column, an accurate description of these processes is especially important.

Clearly, further improvements in the reliability and accuracy of the IGC method depend on the development of more suitable columns to support the stationary phase. Several authors have speculated that the use of capillary columns or open-tube columns would eliminate some of the concerns cited above and would be advantageous for IGC applications.[2,18,19] The principal attraction of an open capillary column is the possibility of achieving more uniform dispersal of the polymeric phase. Ideally, the polymer would cover the wall as a uniform annular film. Such a geometrical configuration would greatly simplify modeling of the transport processes within the column and substantially improve the inherent reliability and accuracy of IGC measurements.

This work provides an experimental demonstration of the use of IGC with uniformly coated capillary columns to study solute diffusion in polymer–solute systems. Although our emphasis is ultimately on the measurement of diffusion coefficients, the use of capillary columns for thermodynamic measurements is also considered.

Models for Capillary Column Chromatography

Because of the early interest in the effect of peak dispersion on separation efficiency for analytical applications, a variety of models for the chromatographic process can be found in the literature. Modeling of capillary column chromatography is a well-developed subject, primarily because the simple geometry frequently leads to models described by analytical solutions.

Early capillary column models, as developed by Golay,[20] Aris,[21] and Khan,[22] evolve from the pioneering work of Taylor,[23] who treated the problem of dispersion in empty capillaries. These efforts produced partial analytical descriptions of the dispersion of a narrow pulse of solute (i.e., expressions for the lower order moments of the concentration distribution). Typically, only the mean residence time and variance about the mean of the distribution can be easily obtained.

The models of Golay and Aris, while useful in providing insight into the mechanisms of peak broadening, are not very useful for extracting diffusion coefficients from experimental data. Golay's model accounts for the effect of solute sorption on dispersion but uses a simplified description of the transport of solute in the stationary phase. Aris treats stationary-phase transport processes in a more rigorous fashion, but his method of solution yields spatial moments (fixed in time) of the concentration distribution. Experimentally, it is convenient only to measure temporal moments. In addition, the method does not afford a simple means of obtaining a real-time concentration distribution. This requires numerical solution of the entire problem.

The model of Khan, based on an approach very similar to those of Taylor and Golay, is more suitable for the analysis of experimental data, as his method leads to temporal moments. Khan also obtains the Laplace transform of the solution, which can be inverted numerically to obtain conveniently the real-time concentration distribution.

In all three models, an attempt is made to account for the dispersion that occurs as the result of coupling between radial diffusion and axial convection in the gas phase (i.e., Taylor dispersion). The inclusion of this effect is a major source of mathematical complexity in the resulting differential equations. A consequence of the nonuniform velocity profile is a nonconstant coefficient in the gas-phase continuity equation. However, in many cases, solute dispersal is determined primarily by the rate of transfer of solute between phases. This, in turn, is often dominated by slow diffusion within the stationary phase. This is particularly true for polymeric stationary phases where the diffusion coefficient in the polymer phase may be 7–10 orders of magnitude smaller than that in the gas phase. For these cases, neglecting gas-phase dispersive processes greatly reduces the mathematical complexity of the problem.

Recognizing this, Edwards and Newman[24] presented a plug-flow model that, in effect, neglects the gas-phase transport processes. They utilize this model primarily to illustrate the effect of polymer-phase diffusion resistance on thermodynamic measurements. In particular, they examined the effect that increasing stationary-phase transport resistance has upon the shift in the time of peak maximum with respect to the mean residence time of a sample. They also show how to use observed shifts in peak maximum from a set of experiments at different carrier velocities to obtain estimates of the stationary-phase diffusion coefficient. While they use Laplace transforms to solve the governing differential equations, they do not generate moment equations in their analysis. Rather, they rely on numerical solutions obtained by inverting the Laplace transform.

Their model is complicated unnecessarily by the use of a cylindrical coordinate system in the description of the stationary-phase transport problem. Even with thickly coated capillary columns, the ratio of coating thickness to column radius is so small as to justify the assumption of

a planar geometry for the coating. They also retain axial diffusion in the polymer-phase transport equation but neglect it in the gas-phase transport equation. In reality, the axial transport of solute within the stationary phase is always negligible in comparison to any other dispersive process. Furthermore, the scheme they describe for extracting the diffusion coefficient is not the most direct or simplest means available (nor did they present it as such).

Noting that further simplifications to the model could be achieved for certain applications, Macris[19] presented a plug-flow model in which curvature of the polymer coating and stationary-phase axial transport are neglected. Using the Laplace transform method, he obtained equations for the lower order moments of the area-averaged concentration distribution, analogous to the results presented by Khan. He used the moment equations to estimate thermodynamic properties from experiments but was not successful in obtaining reliable estimates of the solute diffusion coefficient. For the simplest model investigated, he was also able to define formally an analytical inversion of the Laplace transform and extended the model to include axial molecular diffusion in the gas phase.

In this study, the model proposed by Macris[19] is used to analyze the experimental elution curves. The capillary column is modeled as a straight cylindrical tube with an annular film of polymer deposited on the wall. The following initial assumptions are made:

(1) The system is isothermal.
(2) The carrier gas is greated as an incompressible fluid.
(3) The carrier flow is steady laminar flow with a parabolic velocity profile.
(4) The polymer stationary phase is homogeneous.
(5) The polymer film is constant in thickness.
(6) The polymer film thickness is much less than the radius of the column.
(7) Axial diffusion in the stationary phase is negligible.
(8) The carrier gas is insoluble in the polymer.
(9) The absorption isotherm is linear.
(10) No surface adsorption occurs at the polymer–gas interface or the polymer–column interface.
(11) No chemical reaction occurs between the sample gas and the polymer.
(12) Diffusion coefficients are concentration independent.
(13) The injected sample enters the column as a narrow pulse so that the inlet concentration profile can be modeled as an impulse function.

With these assumptions, the continuity equations for the gas and polymer phase may be written as

$$\frac{\partial c}{\partial t} + 2V(1 - (r/R)^2)\frac{\partial c}{\partial z} = D_g\frac{1}{r}\frac{\partial}{\partial r}r\frac{\partial c}{\partial r} + \frac{\partial^2 c}{\partial z^2} \quad (4)$$

$$\frac{\partial c'}{\partial t} = D_p\frac{1}{r}\frac{\partial}{\partial r}r\frac{\partial c'}{\partial r} \quad (5)$$

where c and c' are the gas-phase and stationary-phase solute concentrations, D_g and D_p are the gas-phase and stationary-phase diffusion coefficients for the solute, z and r are the axial and radial coordinates, and V is the mean velocity of the carrier gas. Appropriate initial and boundary conditions for the problem are

$$c(r,z,t) = c'(r,z,t) = 0 \qquad \text{at } t = 0,\ z > 0 \quad (6)$$

$$c(r,z,t) = \delta(t)c_0 \qquad \text{at } z = 0 \quad (7)$$

$$c(r,z,t) = c'(r,z,t)/K \qquad \text{at } r = R \quad (8)$$

$$D_g(\partial c/\partial r) = D_p(\partial c'/\partial r) \qquad \text{at } r = R \quad (9)$$

$$\partial c/\partial r = 0 \qquad \text{at } r = 0 \quad (10)$$

$$\partial c'/\partial r = 0 \qquad \text{at } r = R + \tau \quad (11)$$

where $\delta(t)$ is the Dirac delta function, c_0 is the strength of the inlet impulse, K is the partition coefficient, R is the radius of the gas–polymer interface, and τ is the thickness of the polymer film.

The problem stated above is sufficiently complex that a closed-form analytical solution in the time domain has not been found. For most practical purposes, the details of the radial distribution of solute are unimportant and a description of the longitudinal dispersion of solute in terms of a local mean concentration (i.e., radially averaged) will suffice. For reasons soon to be apparent, the most mathematically convenient mean concentration is an area-averaged concentration, defined as

$$\mathbf{c} = \left\{\int_0^R rc\ dr\right\} \Big/ \left\{\int_0^R r\ dr\right\} \quad (12)$$

Application of this definition to eq 4, 6, and 7, making use of the boundary conditions given by eq 8 and 9, yields the following:

$$\frac{\partial \mathbf{c}}{\partial t} + \int_0^R \frac{4V}{R^2}(1 - (r/R)^2)\frac{\partial c}{\partial z}r\ dr = D_g\frac{\partial^2 \mathbf{c}}{\partial z^2} + \frac{2D_p}{R}\frac{\partial c'}{\partial r} \quad (13)$$

$$\mathbf{c} = c' = 0 \qquad \text{at } t = 0 \quad (14)$$

$$\mathbf{c} = \delta(t)c_0 \qquad \text{at } z = 0 \quad (15)$$

The equations derived from radial averaging still contain the local concentration as a variable. To proceed further, approximations must be developed to relate the local concentration to the area-averaged concentration. The approach used in earlier models[31,33] was to define a new variable, Δc, which describes the deviation of the local concentration from the mean concentration

$$c(r,z,t) = \mathbf{c}(z,t) + \Delta c(r,z,t) \quad (16)$$

When the chromatographic peak is well dispersed, the radial variation in the gas-phase concentration is expected to be small, so that $\Delta c \ll \mathbf{c}$. This approximation is used with eq 13 and 16 to obtain an approximate solution in terms of $\mathbf{c}$ and its derivatives. That result may then be used to eliminate the local concentration from eq 7 and 13.

A variety of models may be generated by using different assumptions to obtain an approximate solutions of $\Delta c(r,z,t)$. A plug–flow model follows from the simplest approximation for $\Delta c(r,z,t)$, namely that

$$\Delta c(r,z,t) = 0 \quad (17)$$

This is equivalent to stating that the radial gas-phase concentration gradients are sufficiently small that

$$c(r,z,t) = \mathbf{c}(z,t) \quad (18)$$

Substitution of this approximation into eq 13 and evaluation of the integral yield a plug–flow model for the gas phase

$$\frac{\partial \mathbf{c}}{\partial t} + V\frac{\partial \mathbf{c}}{\partial z} = D_g\frac{\partial^2 \mathbf{c}}{\partial z^2} + \frac{2D_p}{R}\frac{\partial c'(r=R)}{\partial r} \quad (19)$$

The interfacial equilibrium boundary condition becomes

$$\mathbf{c}(z,t) = c'(r,z,t)/K \qquad \text{at } r = R \quad (20)$$

The assumption of plug–flow will be valid as long as radial transport processes (molecular diffusion), which tend to smooth out radial concentration variations, occur more rapidly than those processes which create radial concen-

tration variations (i.e., transport across the gas–polymer interface and the coupling of nonuniform axial convection with axial concentration gradients). A more detailed discussion of the implications of this assumption has been given by Edwards and Newman.[24]

The problem is now made dimensionless by introducing the following variables:

$$y = (\mathbf{c}L/c_0V) \qquad x = (z/L) \qquad \eta = (r - R)/\tau$$
$$q = c'L/c_0KV \qquad \theta = Vt/L \tag{21}$$

where L is the length of the column. The transport equations describing the elution process then can be expressed in dimensionless form as

$$\frac{\partial y}{\partial \theta} + \frac{\partial y}{\partial x} = \gamma\frac{\partial^2 y}{\partial x^2} + \frac{2}{\alpha\beta^2}\frac{\partial q(0)}{\partial \eta} \tag{22}$$

$$\frac{\partial q}{\partial \theta} = \frac{1}{\beta^2}\frac{\partial^2 q}{\partial \eta^2} \tag{23}$$

where

$$\alpha = R/K\tau \qquad \gamma = D_g/VL \qquad \beta^2 = \tau^2V/D_pL \tag{24}$$

(Equation 23 has been simplified, recognizing $\tau \ll R$.)

The initial and boundary conditions that remain, written in dimensionless form, are

$$y = q = 0 \qquad \text{at } \theta = 0 \tag{25}$$

$$y = \delta(\theta) \qquad \text{at } x = 0 \tag{26}$$

$$y = q \qquad \text{at } \eta = 0 \tag{27}$$

$$\partial q/\partial \eta = 0 \qquad \text{at } \eta = 1 \tag{28}$$

This pair of coupled linear equations may be solved with Laplace transforms. Solution of eq 22–28 yields

$$Y(s,x) = \exp(1/2\gamma)\exp[-(1/2\gamma)((1 + 4\gamma\Psi(s))^{1/2})x] \tag{29}$$

where

$$\Psi(s) = s + (2s^{1/2}/\alpha\beta)\tanh(\beta s^{1/2})$$

At the exit of the column, where $x = 1$, the solution can be written as

$$Y(s,1) = \exp(1/2\gamma)\exp[-(1/2\gamma)(1 + 4\gamma\Psi(s))^{1/2}] \tag{30}$$

While relatively benign in appearance, this transform is difficult to invert analytically. Following Kubin[25] and Kucera,[26] an inversion scheme using a Hermite polynomial series expansion has been formally defined.[27] It is too cumbersome to be of any practical use. The coefficients are difficult to obtain algebraically, and the series converges slowly.

If real-time concentration profiles are required, numerical inversion of the transform is simpler and more convenient. The theoretical profiles that are presented below were obtained in this manner. A Fourier series approximation method, similar to that presented by Crump,[28] was used. Because a complete elution curve requires inversion of the transform at a large number of time points, a program using a fast Fourier transform algorithm was employed to reduce the computational time. In all cases, series expansions with 4096 terms were used.

An alternate way of obtaining analytical information on the concentration distribution is to make use of the well-known moment-generating property of Laplace transforms.[27] It is readily shown that the various moments of the real-time concentration profile can be related to the transform solution by the following:

$$\mu_k = (-1)^k(L/V)^k \lim_{s\to 0}\frac{d^kY(s)}{ds^k} \tag{31}$$

where

$$\mu_k = \int_0^\infty t^k\mathbf{c}(t)\,dt \Big/ \int_0^\infty \mathbf{c}(t)\,dt \tag{32}$$

The normalized moments can be used to calculate central moments, which are frequently more meaningful in characterizing a distribution

$$\mu_k^* = \int_0^\infty (t - \mu_1)^k\mathbf{c}(t)\,dt \Big/ \int_0^\infty \mathbf{c}(t)\,dt \tag{33}$$

In principle, an infinite number of moments of the distribution could be generated via eq 30 and 31 and then used to reconstruct the real-time distribution. (This is the essence of the inversion scheme presented by Macris.) In practice, the computation of the third and higher moments becomes algebraically cumbersome, except when the transforms are relatively simple in form (in which case they are then likely to be invertible). However, analytical expressions for the first and second moments of a distribution do contain very useful information and frequently can provide a means for parameter estimation from experimental data.

Application of eq 31–33 to the transform solution yields the following pair of moment equations:

$$\mu_1 = (1 + \tau K/R)t_c \tag{34}$$

$$\mu_2^* = \left[\frac{4\tau^3K}{3t_cD_pR} + \frac{2D_gt_c}{L^2}(1 + \tau K/R)^2\right](t_c^2) \tag{35}$$

where $t_c = L/V$, the residence time of the carrier gas.

This pair of equations provides a very basic description of the effect of stationary-phase transport resistance on the characteristics of an elution curve. In particular, note that the dimensionless mean retention time (μ_1/t_c) is independent of the carrier velocity and dependent only upon the thermodynamic properties of the polymer–solute system. This result was also derived by Khan, using his more complicated model.

The dimensionless variance of the distribution (μ_2^*/t_c^2) is a function of both thermodynamic and transport properties of the system. The equation contains two terms. The first represents the contribution of slow stationary-phase diffusion to peak dispersion; the second represents the contribution of axial molecular diffusion in the gas phase. As the solubility of the solute increases or as the diffusion coefficient decreases, greater peak spreading will result. The qualitative effect of increasing values for the polymer-phase diffusion coefficient is illustrated in Figure 1. This diagram shows theoretical elution curves at identical conditions for three values of D_p. As the diffusion coefficient becomes smaller and diffusion into the stationary phase occurs more slowly, the peaks become broader and more skewed. Even a twofold variation in the diffusion coefficient produces a dramatic change in the shape of the outlet profile, indicating that the profile is very sensitive to diffusivity.

Note also that at high carrier gas velocities the dimensionless second moment will be a linear function of velocity, with the slope inversely proportional to the diffusion coefficient. At very low velocities, the dimensionless second moment will be inversely proportional to carrier flow rate and independent of the polymer-phase transport properties. This behavior is qualitatively similar to that

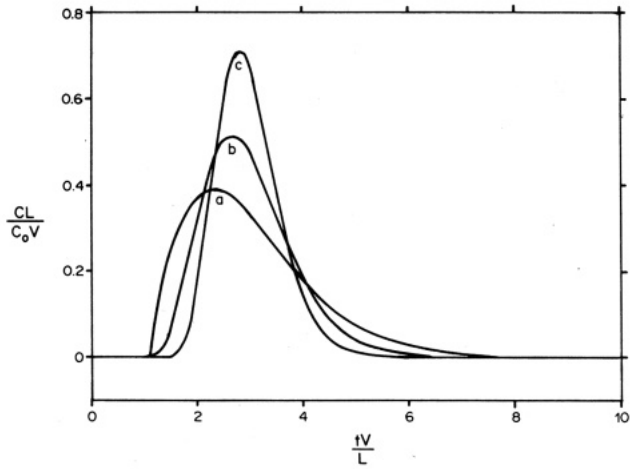

Figure 1. Effect of stationary-phase diffusivity on the elution profile. These theoretical profiles were obtained with $\alpha = 1.0$ and $\gamma = 0.000\,01$; β was varied to show the effect of diffusivity on peak shape. Curve a with $\beta = 1.0$ is the base case. Curve b is for $\beta = 0.707$ or $D_b = 2D_a$. Curve c is for $\beta = 0.5$ or $D_c = 4D_a$.

predicted by the van Deemter equation[14] for packed columns.

Estimation of Model Parameters

The chromatographic experiment analyzed in the previous section can be classified as a pulse-response experiment: the elution curve is the response of the system (i.e., the chromatogram) to an input disturbance, while the Laplace transform given by eq 30 is the transfer function for the system. Methods for obtaining transfer function parameters from system response experiments are well developed and generally fall into one of four categories: time domain fitting, "method of moments", Laplace domain fitting, and Fourier domain fitting.[29] A discussion of the merits of each method for IGC applications is presented by Pawlisch.[30] In this paper, we will restrict analysis to the use of moment methods. In a subsequent paper, we will present a more detailed model and the use of Fourier domain fitting.

The equations needed to apply the moment-fitting procedure are given in the previous section. The first and second central moments of the elution curve are first obtained by numerical integration of the data, following eq 32 and 33. With these data, eq 34 and 35 can then be solved for the diffusion coefficient and partition coefficient (assuming that the other system parameters are known). While parameter estimates may be obtained from a single elution curve, it is preferable to obtain moment data at several different carrier gas flow velocities. The flow-rate dependence of the moment data can then be checked for consistency with the model equations; deviations from expected behavior could indicate flaws in the experimental design or the use of inappropriate modeling assumptions.

When experimental elution curves have been obtained over a range of flow rates, at otherwise constant experimental conditions, the simplest method of data reduction is to fit simultaneously the entire set of moment data to eq 34 and 35. The procedure used in this study is outlined below. For clarity eq 34 and 35 are rearranged in a dimensionless form

$$\mu_1^{\dagger} = \mu_1/t_c = C_1 \tag{36}$$

$$\mu_2^{*\dagger} = \mu_2^*/t_c^2 = C_2(1/t_c) + C_3C_1^2(1/t_c)^{-2} \tag{37}$$

where

$$C_1 = (1 + 2/\alpha) \qquad C_2 = (4/3)\tau^3 K/D_p R \quad C_3 = 2D_g/L^2 \tag{38}$$

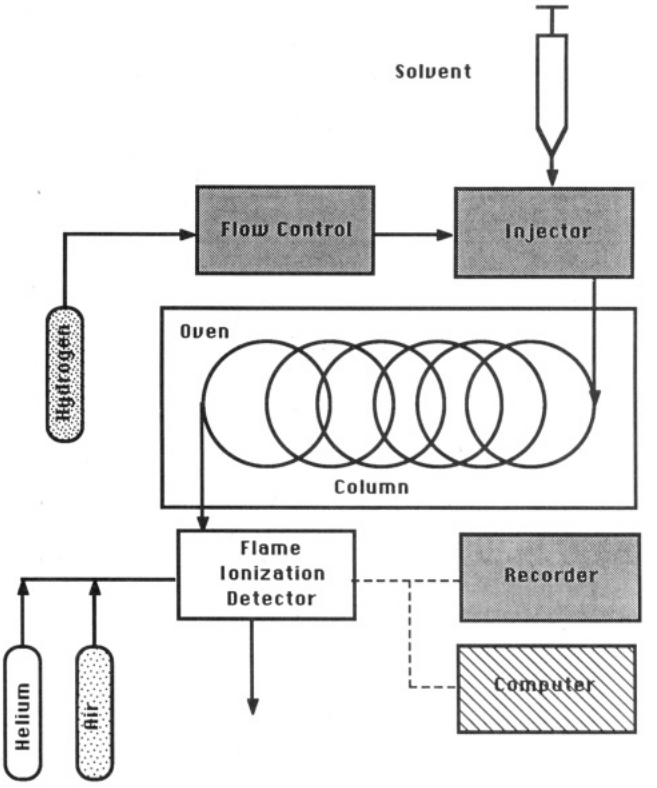

Figure 2. Schematic diagram of apparatus used for inverse gas chromatography.

To obtain an estimate of the partition coefficient, first-moment data were divided by the carrier gas residence time and averaged to find the best estimate for C_1. Individual values of $\mu_1^{\dagger}$ were also plotted vs. carrier velocity to test the result for the flow-rate dependence. An estimate of the diffusion coefficient is obtained by fitting dimensionless second-moment data to eq 37. Under conditions used in this study, the second term in eq 37 is always negligible when compared to the first term. Consequently, plots of dimensionless variance vs. the inverse of the carrier retention time should be linear and extrapolate through the origin. Plots such as this were prepared to test the flow dependence of the data. Linear regression of the data was used to obtain the best estimate of C_2.

Experimental Section

Equipment. The equipment required for inverse gas chromatography is similar to that used in analytical applications. Figure 2 gives a schematic of the apparatus. The chromatograph used in this work was a Varian 3700 (Varian Instruments Division, Palo Alto, CA) equipped with a flame ionization detector (FID), a splitless capillary injector, and a circulating air oven. The chromatograph was designed and equipped specifically for capillary column work. A carrier gas makeup stream, which bypasses the column, provides adequate carrier flow to the detector, the makeup stream is also used to sweep effluent from the column into the detector jet at a high velocity, thus reducing mixing effects at the end of the column. The dead volume of the injector, detector, and connecting lines was negligible in comparison to the column dead volume and did not contribute to peak retention or peak broadening. The oven unit of the Varian 3700 was used without modification. The oven was equipped with a digital control unit that was adjustable in increments of 1.0 °C. A large-diameter, high-speed fan at the back of the oven provided circulation of air to maintain spatial uniformity of temperature. Temperatures within the oven were measured with bare junction copper–constantan thermocouples. Readings at several locations were averaged to obtain the column temperature. Temporal variations in temperature were on the order of 0.1 °C; spatial variations were less than 0.5 °C.

The carrier flow was regulated with a Tylan mass flow controller (Tylan Corp., Carson, CA), capable of regulating flow to ±1% for flows as low as 0.5 mL/min (at ATP). The pressure at the inlet of the column was measured with a Setra Systems pressure transducer (Setra Systems Inc., Natick, MA) that had an accuracy of ±0.05 psi and resolution of ±0.01 psi. Inlet pressures seldom exceeded 16.0 psia. Most of the pressure drop between the column inlet and atmosphere occurs in the detector; considerable pack-pressure develops at the inlet to the flame jet, owing to the large volume of gases that is fed into the flame. The pressure drop across the column itself was estimated to range from 0.05 psi for the slowest flows used to 0.70 psi for the highest flows used.

Data Acquisition. An Apple II microcomputer (Apple Computer, Cupertino, CA) with an Isaac data acquisition system (Cyborg Corp., Newton, MA) was used for recording and integration of the detector output signal. The Isaac unit contains a real-time clock, interval timer, and analog-to-digital (A/D) converter. The microcomputer was used to control the operation of the Isaac and to store, process, and display the elution curves that were recorded.

Data collection of data was started manually by the operator at the time of sample injection. The output signal was scaled so that the maximum detector signal will fall just within the full range of the A/D converter. The signal was sampled at preset, uniform time intervals and converted to a 12-bit binary number, resulting in a digitized signal with a resolution of 0.025% of full scale. The maximum file size for a single elution curve was limited to 1024 data points. In all cases, this provided excellent resolution of the elution profile.

Processing of data files to obtain moment data was done after the experiment was completed. The raw output signals were corrected for base-line offset, i.e., background signal from the detector. This was accomplished with an interactive graphics routine that allowed the operator to shift position of the reference. Once the base-line signal had been adjusted to zero, the lower order moments of the elution curve were calculated, using numerical integration. Data acquisition is discussed in greater detail by Pawlisch.[30]

Preparation of Coated Columns. Preparation of a capillary column with a suitably uniform coating is the crucial step in the implementation of the experiment. Although capillary columns are used frequently in analytical applications, the process of coating is poorly understood. Usual procedures had to be modified to suit the specifications of the experiment. A complete description of the capillary fabrication and coating process is given by Pawlisch.[30] We present an abbreviated outline of the preparation.

Glass capillary columns were drawn from 4 mm × 6 mm Pyrex tubing with a Shimadzu drawing machine (Shimadzu Corp., Kyoto, Japan). Finished columns had coil diameters of 11 cm and a capillary diameter of 0.8 mm. Prior to the coating, the interiors were cleaned with nitric acid and treated with chlorotrimethylsilane. The polymer coating was applied by a static coating technique.[31] A coating solution was filtered and degassed by boiling under reduced pressure to half its original volume. The final concentration of the solution determines the coating thickness. The solution is cooled rapidly and drawn into the column under reduced pressure to hinder redissolution of gases. Once the column has been filled, sufficient additional liquid is drawn through the column to eliminate axial concentration gradients that may have formed as the column was being filled. One end of the column is sealed with a commercial epoxy. After the seal has hardened, the column is mounted in a cascade of constant temperature baths at 35 °C and connected to a vacuum system via the open end. The coating solution is evaporated at nearly full vacuum. If the column has been properly cleaned and sealed, spontaneous boiling will be suppressed, and the coating solution will evaporate at a slow steady rate. The drying process reaches steady state within the first 50 cm of the column; The steady-state drying rate is dependent upon the polymer, solvent, temperature, and solution concentration.

A preliminary assessment of the coating uniformity can be obtained by visual inspection of the coated column. A uniformly coated column and an uncoated column should be nearly identical in appearance (for a glassy or amorphous polymer). Any significant film irregularly acts as a lens for light passing through the column and is readily apparent.

Table I
Summary of Characteristics and Physical Dimensions of Columns

	column		
	1	2	3
coating solvent	THF	THF	chloroform
drying rate, m/day	1.9	8.0	2.5
drying temp, °C	35	35	35
wt of column (coated),	23.603	28.477	20.566
wt of polymer (calcd),	0.472	0.307	0.325
polymer loading $(M_p/M_g) \times 10^2$	2.038	1.089	1.604
std dev, σ	0.042	0.014	0.022
length, cm	1496	1563	1562
av R_0, 10^2 cm	6.29	6.69	5.63
std dev, σ	0.020	0.018	0.014
av R_i/R_0	0.6649	0.6648	0.6436
std dev, s	0.0048	0.0020	0.0020
$(T/T_i)\ \rho_p$, 10^2g/cm^3	2.868	1.533	2.529
std dev, σ	0.097	0.026	0.041
$T\rho_p$, 10^4g/cm^2	11.99	6.82	9.16
std dev, σ	0.34	0.11	0.13

Characterization of Coated Columns. To use the model described earlier, only three column dimensions are needed: average film thickness, average inner radius, and length. For those cases where gas-phase axial dispersion is negligible, only the first two dimensions are needed. In this work, these parameters are determined indirectly, via measurements of the column and coating weight and accessible physical dimensions of the column; uniformity is confirmed by examination of column fragments with a scanning electron microscope (SEM). An extensive discussion of the column and film characterization is given by Pawlisch.[30] We present a summary of the results and a brief description of the analytical procedure.

Three columns were used for this study. All three were prepared by the procedures described above. Tetrahydrofuran was used as a coating solvent for two of the columns; chloroform was used for the third. These had film thicknesses of approximately 12, 7, and 9 μm and will be designated columns 1, 2, and 3, respectively, with reference to the order in which they were used. The pertinent physical dimensions of the columns are given in Table I. Because film thickness is dependent on the polymer density, the film thickness will vary with the temperature of the experiment. For this reason, the film dimensions in Table I are reported as the product of the film thickness with the polymer density.

The procedures used to characterize the column required destruction of the column. The column was first weighed to obtain a total coated weight and then broken into several segments of approximately equal length. At each point where the column is broken, very short pieces were retained for examination with an SEM. The polymer loading (i.e., ratio of polymer mass to column mass, r_m) for each column segment was determined from the weight of the sample before and after polymer removal. The average outside diameter of each segment was determined by making measurements with a precision micrometer at a large number of places along the length of the segment. Weight, length, and diameter measurements on shorter pieces of each segment were then used to calculate the characteristic ratio of inner to outer diameter of the column. On the basis of the kinematics of the drawing process, this ratio should be constant for a given column. The above information is sufficient to calculate the average inner diameter and coating thickness for each column segment. The average coating thickness and inner diameter for the entire column are obtained from the individual segment measurements. If the length of the column is needed it can be calculated from the mass of the column and average inner and outer diameters.

In each column, the variability of segment coating thickness measurements was less than ±1.25%, indicating that the axial distribution was uniform. Uniformity of the coating was verified by direct examination of the column samples using an ETEC U-1 scanning electron microscope. In virtually all samples, the polymer was deposited on the wall as a smooth, continuous, annular film. Adhesion of the film to the wall appeared to be good. A micro-

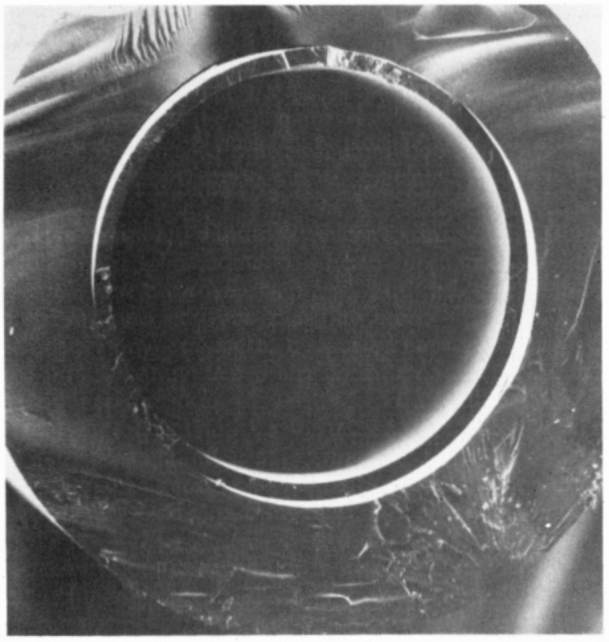

Figure 3. Cross-sectional micrograph of a polystyrene-coated capillary column. Film thickness is approximately 35 μm.

graph of a typical column cross section is shown in Figure 3.

Materials. The polystyrene used for this work was a commercial-grade polymer (Lustrex Crystal) obtained from the Monsanto Co. (St. Louis, MO). The number- and weight-average molecular weights of the polymer, as determined by gel permeation chromatography, were 120000 and 266000, respectively. Benzene and toluene were spectral-grade products of 99.9% purity, obtained from MCB Manufacturing Chemists, Inc. (a division of EM Industries, Inc., Gibbstown, NJ). Ethylbenzene was Certified grade, obtained by Fisher Scientific Co. (Fair Lawn, NJ). Gases used for the operation of the chromatograph were supplied by the Linde Division of the Union Carbide Corp. A high-purity, chromatographic-grade helium was used as the carrier gas. Dry-grade air and hydrogen were used for the flame ionization detector.

Experimental Procedure. Freshly coated columns must first be conditioned to remove any residual coating solvent. This is done after the column is installed in the oven. Carrier flow is started and the oven temperature is raised gradually over a period of hours, allowing adequate time for residual solvent to diffuse out of the polymer coating. The column was ready for use when a drift-free base line was observed.

The procedure for obtaining an elution curve is very simple. After the GC reached stable, steady-state operation, a small amount of solvent was injected into the carrier gas. The amount of solvent in the carrier gas leaving out of the column was measured with a flame ionization detector. At constant carrier gas flow, the magnitude of the FID signal, with respect to the base-line value, is proportional to the concentration of solvent in the carrier gas. Elution curves are reported with an on-line microcomputer, as described earlier. Each elution curve is analyzed to obtain the mean residence time, the variance, the median residence time, and the time to maximum solute concentration. The latter two times have no special theoretical significance. They are often used in conventional IGC studies as measures of peak retention and were obtained here only for comparison.[2]

Liquid and vapor solvent samples were injected into the carrier gas using a sampling syringe and a standard splitless capillary injection system. The injector block was maintained at least 50 °C above the normal boiling point of the solute to ensure rapid vaporization of liquid samples. The relative merits of different syringe designs and injection procedures are discussed by Pawlisch.[30] For most experiments, liquid samples with a volumn of 0.01 μL were used to ensure that solute elution occurred at conditions approaching infinite dilution in the stationary phase. The assumption of infinite dilution was verified by additional experiments, which showed that the results were independent of sample size.

Table II
Summary of Experimental Conditions

temp, °C	column	approx carrier velocity, cm/s			
		Benzene as Solvent			
110	2	2.00	2.65	4.10	
120.1	1	2.65	3.50	5.00	
120.2	2	3.20	4.60	7.65	
130.2	1	3.20	5.00	9.25	
130.4	2	4.25	6.00	7.30	8.80
130.2	3	5.50	7.80	14.40	24.60
140.6	2	5.35	7.60	11.80	
		Toluene as Solvent			
110	2	2.00	2.65	4.10	
120.1	1	2.65	3.50	5.00	
120.2	2	3.20	4.60	7.65	
130.2	1	3.20	5.00	9.25	
130.4	2	4.25	6.00	7.30	8.80
130.2	3	5.50	7.80	14.40	24.60
140.6	2	5.35	7.60	11.80	
		Ethylbenzene as Solvent			
110	2	2.00	2.65	4.10	
120.1	1	2.65	3.50	5.00	
120.2	2	3.20	4.60	7.65	
130.2	1	3.20	5.00	9.25	
130.4	2	4.25	6.00	7.30	8.80
130.2	3	5.50	7.80	14.40	24.60
140.6	2	5.35	7.60	11.80	

Carrier gas velocity is determined from the elution time of methane samples, which do not interact with the polymer coating to any appreciable extent. Measurement of other experimental parameters is discussed under Equipment.

Results and Discussion

Overview. The capillary-column IGC technique was used to study the partition coefficients and diffusion coefficients of benzene, toluene, and ethylbenzene in polystyrene, from 110 to 140 °C. These systems have been thoroughly investigated by other techniques (specific studies will be cited later), thus allowing for direct comparison of capillary-column IGC with other methods. Measurements for each solvent–polymer pair were obtained at several carrier flow rates, using each of the three columns previously described. Table II contains a summary of the experiments. Two or three replicate elution curves were obtained at each of the conditions listed. The use of multiple columns and several flow rates was intended to provide for checks of the validity of the theoretical model used for parameter estimation. In the discussion that follows, all experiments within a row in Table II are considered part of the same data set. Each data set was used to obtain a diffusion coefficient and partition coefficient, using the data reduction procedure outlined earlier. Tests of the flow dependence of the moment data were also performed for each data set to evaluate the suitability of the theoretical model. Tests to evaluate the model are discussed first, followed by a comparison of the results to the literature.

Tests of the Model. Peak Retention. According to eq 46, the dimensionless retention time should be independent of the carrier gas velocity for a given column and solvent. To verify this, plots of dimensionless retention time vs. $1/t_c$ were prepared for each data set, and statistical tests for correlation were performed. In general, these tests confirmed that the dimensionless retention time was independent of carrier flow.

The flow dependence of the first moment data is illustrated by Figure 4, which shows normalized data for toluene at 130 °C with column 1. For comparison, data for the median elution time of the sample and the time of the elution curve maximum are also shown (see discussion

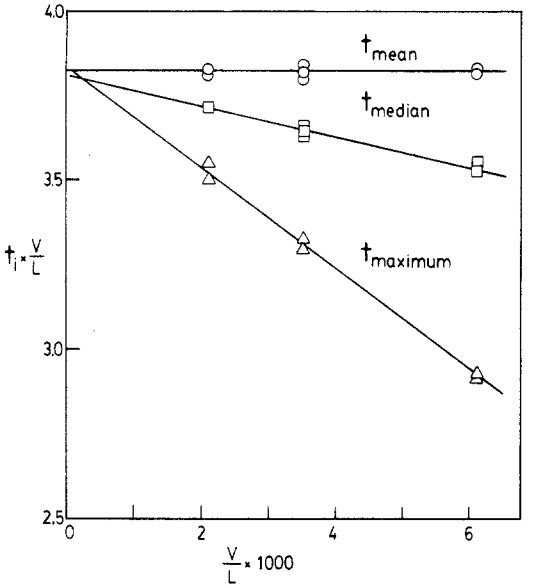

Figure 4. Dimensionless peak retention time vs. flow rate. Data for toluene at 130 °C from column 1 are shown. Plotted are the dimensionless mean time, median time, and time of peak maximum.

below). Plots for other data sets were qualitatively similar in appearance. In most of the data sets, dimensionless retention times were constant to ±2%. Exceptions to this were some of the lowest temperature data sets obtained with column 2, where the variability was as high as ±5%. The poorer reproducibility of those runs is attributed to injection problems associated with a specific design of sampling syringe.[30]

Despite the good reproducibility of the data, a weak correlation between dimensionless retention time and carrier velocity appears to be present in many of the data sets. In general, data from 110 to 120 °C show a slight decrease in dimensionless retention time with decreasing carrier velocity. At higher temperatures, a slight increase in retention time with decreasing velocity was sometimes seen. The slope of the data, as determined by linear regression, is largest at the lowest temperature and becomes progressively less pronounced as the temperature increases. In the majority of the cases, this dependence is not statistically significant (using 95% confidence limits). Exceptions to this were the lowest temperature experiments (120 °C) done with column 1. It should be noted that even when the correlation with flow rate is statistically significant, the magnitude of the variation is still small. For the data sets obtained at 120 °C with column 1, linear extrapolation to zero carrier velocity yields a retention time which is only 2% to 3% lower than a mean value for the data set.

We attribute the flow-rate dependence to systematic errors in the determination of the mean residence time for asymmetric, strongly tailed elution curves. As noted earlier, the elution curves obtained in the study were always superimposed on a background or base-line signal. In order to correctly calculate the moments of the distribution, the output signal must be corrected for the offset of the base-line signal from zero. That is, the elution curve is integrated with respect to a hypothetical zero concentration base line that is superimposed on the elution curve. In the present study, a linear base-line correction, based on the detector signal at the beginning and end of the experiments, is used. Unfortunately, because of random signal noise and base-line drift, correct application of base-line correction may be problematic. The sensitivity of first-moment calculations to base-line placement depends primarily on the shape of the elution curve. Peaks that are nearly symmetric, with short tails, yield the most reliable results: If the base-line correction is too large or too small, the integration error on the leading edge of the distribution tends to be counterbalanced by a similar error on the trailing edge. When the elution curve is highly asymmetric, with a long tail, the mean residence time is more strongly affected by the trailing edge of the peak. Improper base-line correction can change significantly the magnitude and extent of the tail, thus producing noticeable shifts in the calculated mean.

In the present study, the asymmetry of the elution curves increases as the column temperature decreases, consistent with a strong temperature dependence of the diffusion coefficient (see Figure 1). Thus, the higher variability and stronger flow dependence of the first-moment data for lower temperature data sets are consistent with the above explanation.

Other Retention Measures. In addition to the mean residence time, the median residence time and time of maximum concentration were determined for each elution curve. It is common practice in packed-column chromatography to use these characteristics as a measure of peak retention. The principal justification is that these quantities are easier to measure and, for a perfectly symmetric elution curve, are identical with the mean retention time. However, if strong mass-transfer resistances are present, these other measures of peak retention may be inappropriate for calculation of the partition coefficient. Thus, when these other measures of retention time are used, retention data are sometimes extrapolated to zero flow rate to reduce the significance of mass-transport limitations.[12,32]

In the present study, the median time and time of peak maximum were always less than the mean residence time. As illustrated by Figure 4, the differences were sometimes quite large, owing to the highly asymmetric shape of some of the elution curves. For most data sets, the deviation of the median retention time from the mean time was linear. Extrapolation of mean and median retention times to zero flow rate usually yields the same value, within experimental error. The deviation of the maximum time data from the mean time was not always linear. The maximum time plots were often strongly curved, making extrapolation to zero flow rate difficult. These results suggest that for thickly coated columns that yield highly skewed elution curves use of the time of maximum concentration as a measure of peak retention can lead to serious errors in thermodynamic property estimates. Lichtenthaler et al.[18] report difficulties in an earlier study using capillary columns to obtain thermodynamic measurements.

Peak Broadening. Equation 37 shows that at sufficiently high carrier flow rates ($t_c \rightarrow 0$) the dimensionless second moment should be proportional to the carrier velocity (i.e., μ_2^*/t_c is constant). For the conditions used in this study, the second term on the right-hand side of eq 37 is always negligible in comparison to the first term. Consequently, a plot of dimensionless variance vs. carrier velocity should be linear and extrapolate through the origin. To verify this, plots were prepared for each data set and the correlation of μ_2^*/t_c with carrier velocity was tested statistically. In general, the second-moment data show the theoretically expected behavior.

The dependence of the dimensionless variance on flow rate is typified by Figure 5, which shows data for toluene from column 1 at 120 and 130 °C. All the data sets are similar in nature, being fit adequately by a straight line

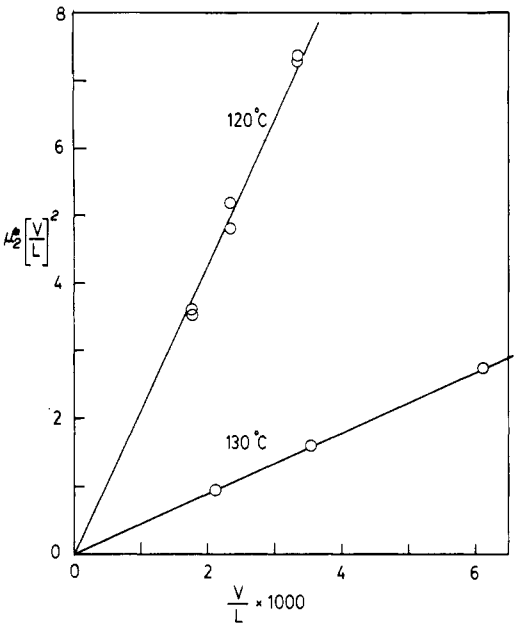

Figure 5. Dimensionless peak variance vs. flow rate. Data for toluene at 120 and 130 °C from column 1 are shown.

passing through the origin. The two-parameter regression line fitted to each data set always had an intercept value near zero and did not differ significantly from the one-parameter regression line constrained to pass through the origin. For most data sets, the slopes of the two regression lines differed by less than 10%. The worst agreement was obtained with toluene in column 2 at 130 °C, where the slopes were different by 30%. However, because of the larger scatter in this data set, the difference between the two lines was not statistically significant (at a 90% confidence limit).

As might be expected from the above observations, most of the data sets show no correlation (using 90% confidence limits) between μ_2^*/t_c and the carrier velocity. Exceptions were the data sets from column 1 at 120 °C and the toluene data set from column 2 at 110 °C. Not coincidentally, these are the same data sets that showed the strongest correlation between the dimensionless mean retention time and the carrier velocity.

The weak flow dependence is again believe to be an artifact of errors in the placement of the reference base line. As in the case of the first-moment calculations, any error in the selection of the base line used for the integration of the peak will result in errors in the calculation of the variance. Because of the nature of the weighting function, the value of the second central moment of a distribution is even more strongly dependent than the first moment on data in the tail of the distribution. Thus, the accuracy of the second-moment calculations is even more sensitive to base-line placement, especially when the concentration distribution is asymmetric and strongly tailed. As noted before, the data sets that show the strongest flow dependence were those in which the elution curves were strongly tailed.

Comparison of Real and Theoretical Elution Curves. One disadvantage of the method of moments for parameter estimation is that the procedure is not model discriminatory; distributions that have radically different shapes can have identical first and second moments. It is always advisable to confirm that the parameter estimates obtained from a moment analysis will correctly reproduce the original elution curves. Such comparisons are shown in Figure 6 for elution curves obtained at several different flow rates with toluene in column 1 at 130 °C. In these

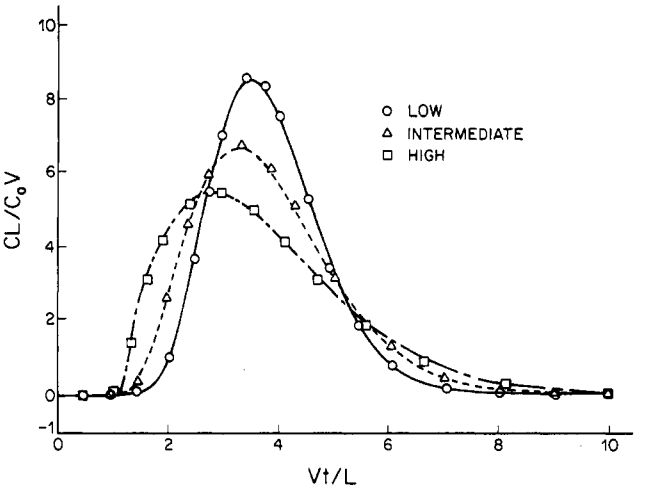

Figure 6. Comparison of theoretical and experimental elution curves for toluene from the column at 130 °C at three carrier velocities. Experimental data are indicated by the solid points. The theoretical profile, indicated by the solid line, was generated with the best set of parameter estimates obtained by moment fitting.

Table III
Summary of Thermodynamic Interaction Parameters (Obtained by Moment Fitting)

solvent	temp, °C	column	retention vol	Ω_1^∞ (σ)	χ_{12} (σ)
benzene	110	2	30.6 (0.7)	4.33 (0.09)	0.205 (0.022)
	120.1	1	23.1 (0.8)	4.52 (0.16)	0.238 (0.035)
	120.2	2	24.3 (1.0)	4.29 (0.18)	0.185 (0.042)
	130.2	1	18.1 (0.6)	4.61 (0.16)	0.247 (0.034)
	130.4	2	18.4 (0.4)	4.51 (0.11)	0.224 (0.024)
	130.2	3	17.9 (0.4)	4.66 (0.11)	0.257 (0.023)
	140.6	2	14.6 (0.5)	4.63 (0.16)	0.239 (0.034)
toluene	110	2	61.9 (2.8)	4.17 (0.19)	0.162 (0.045)
	120.1	1	43.7 (1.5)	4.49 (0.16)	0.227 (0.035)
	120.2	2	45.3 (2.3)	4.32 (0.22)	0.188 (0.051)
	130.2	1	33.3 (1.1)	4.56 (0.16)	0.233 (0.034)
	130.4	2	34.1 (1.0)	4.43 (0.13)	0.211 (0.029)
	130.2	3	34.0 (0.9)	4.46 (0.12)	0.211 (0.026)
	140.6	2	25.5 (0.6)	4.66 (0.10)	0.245 (0.022)
ethyl-benzene	110	2	110.1 (5.6)	4.25 (0.22)	0.188 (0.051)
	120.1	1	74.6 (2.6)	4.62 (0.16)	0.264 (0.035)
	120.2	2	77.8 (1.6)	4.42 (0.09)	0.220 (0.020)
	130.2	1	55.9 (2.1)	4.63 (0.17)	0.258 (0.037)
	130.4	2	56.4 (1.7)	4.57 (0.14)	0.245 (0.030)
	130.2	3	56.2 (1.4)	4.61 (0.12)	0.254 (0.025)
	140.6	2	42.2 (1.0)	4.66 (0.11)	0.256 (0.023)

diagrams, the points are taken from experimental elution curves, while the solid lines are theoretical elution curves generated with values of α and β obtained from moment measurements. Inversion of the Laplace transform solution was done numerically with a Fourier series method.[28]

Clearly, the parameters obtained from the moment analysis will reproduce the original elution curves, indicating that reliable estimates have been obtained. The fact that the experimental elution curves are accurately reproduced over a range of carrier velocities with a single set of parameters, K and D_p, is evidence that the theoretical model accurately describes the elution process. Comparisons of theoretical and experimental curves for a number of other cases showed similar agreement.

Summary of Parameter Estimates. Table III gives a summary of the partition and diffusion coefficient estimates obtained from each data set using the moment-fitting procedures described earlier. The number in parentheses following each table entry is an estimate of the standard deviation of the measurement, based on the accuracy of the column dimensions and the reproducibility

Table IV
Linear Regression of the Activity Coefficient Data as a Function of Temperature (Based on Moment Data)

solvent	mean value (σ)	regression coeff	intercept	corr coeff
benzene	4.51 (0.15)	0.0116	3.04	0.793
toluene	4.44 (0.16)	0.0143	2.64	0.89
ethylbenzene	4.54 (0.15)	0.0125	2.96	0.836

of the moment measurements.[30] Note that the data taken at 120 and 130 °C can be compared to check the column-to-column reproducibility of the results. Within the estimated experimental error, there is agreement among the data. Since the surface-to-volume ratio of the polymer coating is difficult in each column, the consistency of the data is evidence that surface sorption was not significant.

Other Thermodynamic Interaction Parameters. Partition coefficient data are seldom reported in the literature dealing with polymer solution thermodynamics. To facilitate comparisons with other studies, partition coefficient data from the present study were used to calculate more common thermodynamic interaction parameters such as the specific retention volume, the infinite dilution activity coefficient, and the Flory–Huggins interaction parameter.

The specific retention volume is related to the partition coefficient through the following definition:[1]

$$V_g^0 = 273.2K/T\rho_p \tag{39}$$

where V_g^0 is the specific retention volume, T is the column temperature, and ρ_p is the density of the polymer. The infinite dilution activity coefficient is related to the specific retention volume by the following:[3]

$$\ln (a_1/w_1) = \ln \Omega_1^\infty = \ln \frac{273.15\mathbf{R}}{p_1^0 V_g^0 M_1} - \frac{p_1^0(B_{11} - V_1)}{\mathbf{R}T} \tag{40}$$

where $\mathbf{R}$ is the ideal gas constant, M_1 is the molecular weight of the solute, B_{11} is the second virial coefficient, V_1 is the molar volume of the solute, and p_1^0 is the vapor pressure of the solute. Note that, following the widely used convention of Patterson et al.,[33] a weight-fraction activity coefficient is used.

The Flory–Huggins interaction parameter is related to the weight-fraction activity coefficient by the following:[4]

$$\ln \Omega_1^\infty = \ln (v_1/v_2) + (1 - V_1/M_2 v_2) + \chi_{12} \tag{41}$$

where v_i is the specific volume of component i, M is the number-average molecular weight of the polymer, and χ_{12} is the Flory–Huggins interaction parameter. For a high molecular weight polymer, this equation simplifies to

$$\ln \Omega_1^\infty = \ln (v_1/v_2) + 1 + \chi_{12} \tag{42}$$

These equations, along with appropriate physical property data,[30] are used to obtain the results shown in Table III. The number in parentheses is the estimated standard deviation of the measurement.

As expected, the specific retention volume data varies with temperature. For all three solvents, the retention volume diagrams are linear. In Figure 7, the data have been plotted on a retention diagram (i.e., logarithm of retention volume vs. the reciprocal of the absolute temperature) to illustrate the temperature dependence. Such plots are normally linear, except in the vicinity of a phase transition such as the melting point or glass transition temperature, where discontinuities in the slope may occur.[1] In the present study, linear diagrams were obtained for all three solvents over the temperature range studied.

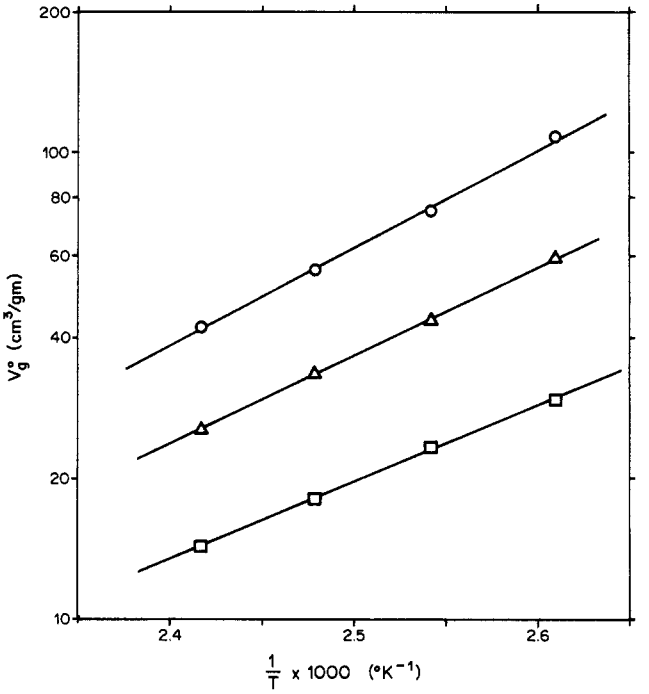

Figure 7. Retention volume diagram for benzene, toluene, and ethylbenzene.

Linearity of the retention diagrams is unusual in that the lowest temperature used in this study is very close to the glass transition temperature of polystyrene (~100 °C). In previous IGC studies, it has been observed that retention diagrams are frequently curved at temperatures slightly above the glass transition and that linear behavior is not expected unless the column temperature is at least 30–50 °C above the glass transition of the polymer. This nonideal behavior has been attributed to a change in the retention mechanism as the polymer changes from a liquid to a glass: Well above the glass transition, retention volume is determined by bulk sorption, while below the glass transition, the solvent is not able to penetrate the polymer, and surface sorption is the dominant mechanism.

Several studies have shown that departure from linearity at temperatures just above the glass transition is a consequence of using the time of peak maximum as a measure of peak retention.[24,40,41] Near the glass transition of a polymeric stationary phase, a dramatic decrease in the stationary-phase diffusion coefficient often occurs. Hindered transport of the solute within the stationary phase produces substantial skewing of the peak, so the time of peak maximum no longer provides an accurate measure of the solute–polymer interaction. The shift in the time of peak maximum with respect to the true retention time of the peak causes curvature of the retention volume plot. In the present work, such difficulties are avoided by using the mean retention time as the measure of peak retention.

The data for the infinite activity coefficient and Flory–Huggins interaction parameter are nearly constant for each solvent over the range of temperature used in the study. Statistical tests of the activity coefficient data do show a positive correlation with temperature. The correlation is significant (using 95% confidence limits) for all solvents, indicating an increase in activity coefficient with temperature. All three solvents have infinite dilution activity coefficients and Flory–Huggins interaction parameters of similar magnitude.

Comparisons with Literature Data. Thermodynamic Data from Packed-Column IGC. Table V lists

Table V
Packed-Column IGC Studies of Aromatic Solvents with Polystyrene

symbol	investigation	M_n	M_w
●	this study	120 000	266 000
○	ref 35	50 660	53 700
▲	ref 36	20 000	not available
■	ref 12	76 000	82 100
△	ref 32	97 600	100 500
▽	ref 37	not available	not available
□	ref 38	9 600	97 600

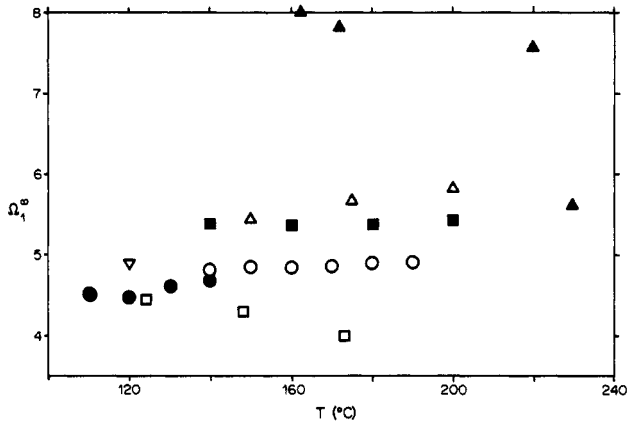

Figure 8. IGC data for infinite dilution activity coefficient of benzene in polystyrene. Data from this study are compared with data from packed-column studies. Key to symbols is given in Table V.

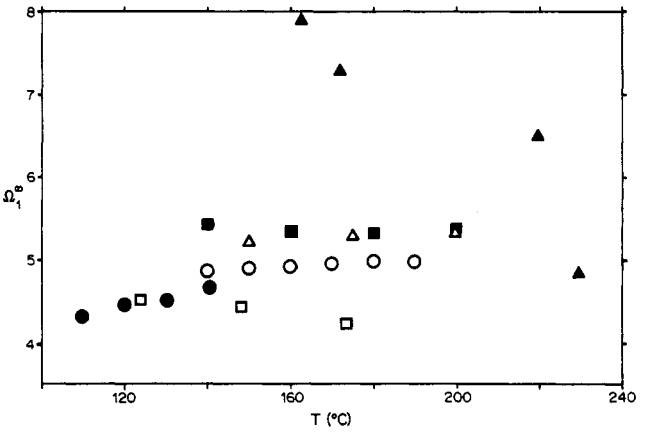

Figure 9. IGC data for infinite dilution activity coefficient of toluene in polystyrene. Data from this study are compared with data from packed-column studies. Key to symbols is given in Table V.

a number of previous studies that used packed-column IGC to obtain solution thermodynamics data for the systems under consideration in this study. Infinite dilution activity coefficients taken from these references are compared to the results of the present study in Figures 8–10. It is clear from these comparisons that the results of the present study fall within the range of data reported by earlier studies. It is also apparent, however, that the agreement among the results of the earlier studies is only fair. For example, for benzene and toluene at 170 °C, the reported activity coefficient ranges from 4.5 to 8.0. The data of Covitz and King[38] and Gunduz and Dinçer[36] are in particularly poor agreement with the rest of the studies and probably should be disregarded. The remaining data generally fall between 4.5 and 5.5, depending on the study and solvent. The activity coefficient data obtained in the present study are somewhat lower, on average, than the majority of the other data. The significance of this difference is difficult to evaluate given the range of values reported in the other studies. There are a number of differences between the present work and earlier studies which should be taken into consideration when comparing the current data with the results of the earlier studies.

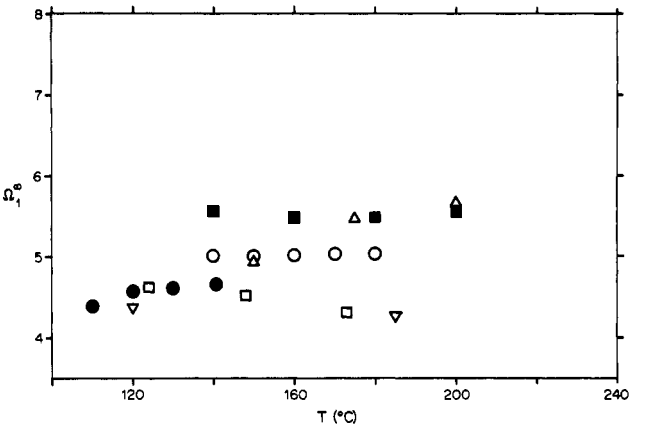

Figure 10. IGC data for infinite dilution activity coefficient of ethylbenzene in polystyrene. Data from this study are compared with data from packed-column studies. Key to symbols is given in Table V.

Since the temperatures used in this study are somewhat lower than in the previous studies, the lower values might simply be a consequence of the temperature dependence of the activity coefficient. When the data from previous studies are viewed as a group (excluding data from ref 36 and 38), they do suggest a weak positive temperature dependence for the activity coefficient. A similar trend is seen in the results of this work. However, the temperature dependencies of individual studies are inconsistent. Some studies show a definite increase of the activity coefficient, while others show no effect or a slight decrease.

It should be noted that there are differences among the studies in the molecular weight of the polymer used (see Table V). In the present study, the polymer had a number-average molecular weight of 120 000 and a broad molecular weight distribution; in earlier work, narrow molecular weight distribution polymers with number-average molecular weights ranging from 50 000 to 100 000 were used. It is unclear what effect molecular weight and molecular weight distribution will have on thermodynamic interaction parameters. Covitz and King[38] report small, but consistent changes in activity with changes in molecular weight, while Newman and Prausnitz[32] report no significant differences.

A third difference between this work and the earlier studies is the use of a relatively thick polymer coating. In most packed-column work, the mean film thickness rarely exceeds 0.5 μm, while in the present study the film thickness is 10–20 times greater. Thus, in the present study, the ratio of surface area to polymer mass is considerably smaller than in most packed-column studies. If significant surface sorption were to occur, specific retention volumes measured in a packed column would be larger than specific retention volumes measured in a capillary column. Consequently, the activity coefficients measured in the packed column would be lower than activity coefficients measured in the capillary column. As noted above, the opposite was observed.

The use of relatively thick column coatings also addresses a concern raised by Lichtenthaler et al.,[18] who have suggested that thermodynamic properties measured by packed-column IGC may not be representative of bulk polymer owing to the low mean film thickness. Others have disputed this claim, arguing that the mean coating

thickness in a packed column is usually large enough to guarantee that bulk properties are measured.[39] The issue remains unresolved.

The final difference between this work and earlier packed-column studies is the manner in which retention volumes were measured. In the present study, the mean residence time of the sample, which is the theoretically correct measure of peak retention, was used to calculate retention volume. In the other studies (excluding ref 47), the time of maximum solute concentration is used.

As discussed earlier, the time of peak maximum corresponds to the true retention time of the peak only when mass-transfer resistances are negligible. It is well-known that mass-transfer resistances will cause skewing of the elution curve and that such skewing will cause the retention volume, as determined from the time of peak maximum, to be underestimated.[24,40-42] The absence of significant mass-transfer resistances is normally established by demonstrating that measured retention volumes are independent of carrier flow and verifying that the elution curves are symmetric.[1,2]

It is significant to note that in two of the studies listed in Table V, retention volume data were found to be dependent on carrier velocity.[12,32] In these studies, the retention volume data were extrapolated to zero velocity to minimize the effect of mass-transfer resistances. There is no theoretical reason to believe that such a procedure will always work; in the present study, where strong mass-transfer resistances were present, extrapolation of peak maximum data to zero carrier velocity often produced significant errors in measured retention volume.

In two of the other studies cited, no effort was made to check for flow dependence of the retention data.[36,37] The judgement that mass-transfer resistances were negligible was based entirely on the observation that the elution curves were symmetric. This may not be sufficient to ensure that equilibrium retention volume measurements have been obtained.

In a subsequent paper, we will show that variations or irregularities in the coating thickness will enhance the skewing associated with mass-transfer resistance in the stationary phase. In essence, as the coating becomes more irregular, portions of the polymer become less accessible to the solute. Although the mean residence time of the solute does not change, any solute that penetrates into a thicker portion of the film will remain trapped for a longer period of time. Consequently, the elution curve develops a long, flat tail.

We speculate that if the distribution of polymer is sufficiently irregular, this tail might fall below the resolution of the detector and thus disappear. For practical purposes, some fraction of the polymer is then completely inaccessible to the solute and would not contribute to the measured retention time. It is conceivable that in some circumstances the elution curve might even appear to by symmetric. Such a phenomenon would explain the inconsistencies in the temperature dependence of activity coefficient data from the cited studies. Because the stationary-phase diffusion coefficient is so temperature dependent, changes in the column temperature would radically alter the accessibility of any deep pools of polymer that are present.

Thermodynamic Data from Vapor Sorption. Studies in which vapor sorption techniques have been used to measure thermodynamic properties of molten polystyrene are limited in number. The best data available for the solvents used in the present work are those of Vrentas, Duda, and Hsieh.[8] Using a quartz spring balance, they measured the solubility of benzene, toluene, and ethylbenzene in a sample of commercial polystyrene over a range of temperature (115–117 °C) and solute partial pressure (up to 1 atm). They do not report solubility or activity coefficient data directly. Instead, they use the Flory–Huggins polymer solution model to correlate the data and obtain an estimate of the Flory–Huggins interaction parameter using a nonlinear regression analysis. They also used the Flory–Huggins theory (i.e., eq 41) to predict infinite dilution activity coefficients from interaction parameters measured by vapor sorption at finite solute concentrations.

Table VI
Comparison of Flory–Huggins Interaction Parameters from This Study to Data from Earlier Vapor Sorption Studies

solvent	mean value from this study	mean value from vapor sorption
benzene	0.23 (0.03)	0.30 (0.01)
toluene	0.21 (0.03)	0.29 (0.01)
ethylbenzene	0.24 (0.03)	0.35 (0.01)

Table VII
Comparison of Infinite Dilution Activity Coefficients from This Study with Data Predicted by the Flory–Huggins Interaction Parameters from Vapor Sorption Studies

solvent	temp, °C	regression line prediction for IGC data	predicted by vapor sorption
benzene	110	4.32	4.76
	120	4.44	4.81
	130	4.55	4.86
	140	4.67	4.92
toluene	110	4.21	4.74
	120	4.36	4.78
	130	4.5	4.82
	140	4.64	4.87
ethylbenzene	110	4.34	5
	120	4.46	5.04
	130	4.59	5.07
	140	4.71	5.12

Table VI compares the Flory–Huggins interaction parameters obtained by the present study with the vapor sorption data reported by Duda et al. The values obtained by IGC are about 30% lower than those measured by vapor sorption, while the ranking of the solvents according to the value of χ_{12} is the same in both studies. Table VII compares infinite dilution activity coefficient data from the present study to values calculated from the interaction parameter data reported by Duda et al. As would be expected from the differences in χ_{12}, the activity coefficients predicted from vapor sorption are about 10% higher than the data obtained in the present study.

We can offer no convincing explanation of the apparent disagreement between the two studies. The polymer samples used had similar characteristics: in both studies, the polymer had been produced commercially and the weight average molecular weights were similar (~270 000). Different temperature ranges were used in each study, but there was considerable overlap. (IGC data were obtained between 110 and 140 °C, while vapor sorption data was obtained between 115 and 170 °C.) The only major difference between the studies (aside from the measurement technique) is the solvent concentration at which the data were obtained: the vapor sorption measurements were made at low, but finite concentrations of solvent, while the IGC measurements were made under conditions at which the solvent concentration approaches infinite dilution. Certainly, if χ_{12} were concentration dependent, then a

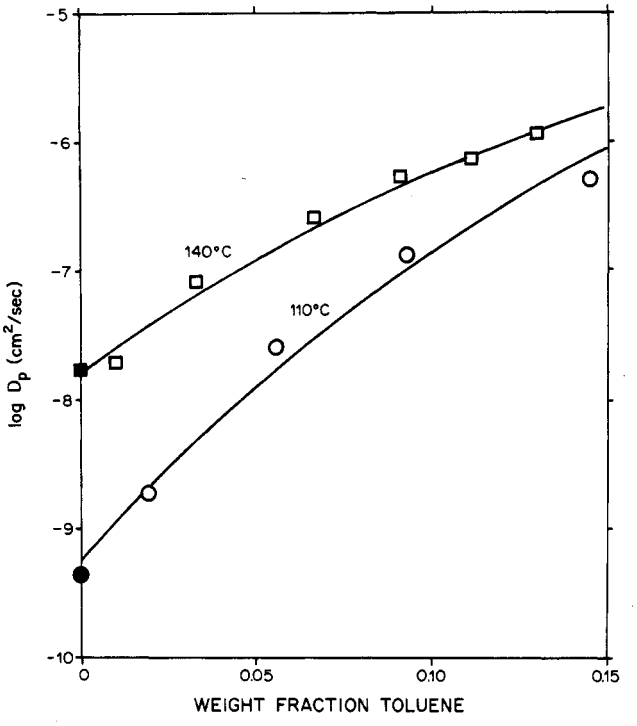

Figure 11. Comparison of IGC and vapor sorption data for the diffusivity of toluene in polystyrene. Solid symbols indicate infinite dilution diffusivities determined by IGC. The open symbols indicate vapor sorption measurements reported by Duda et al.[43,44]

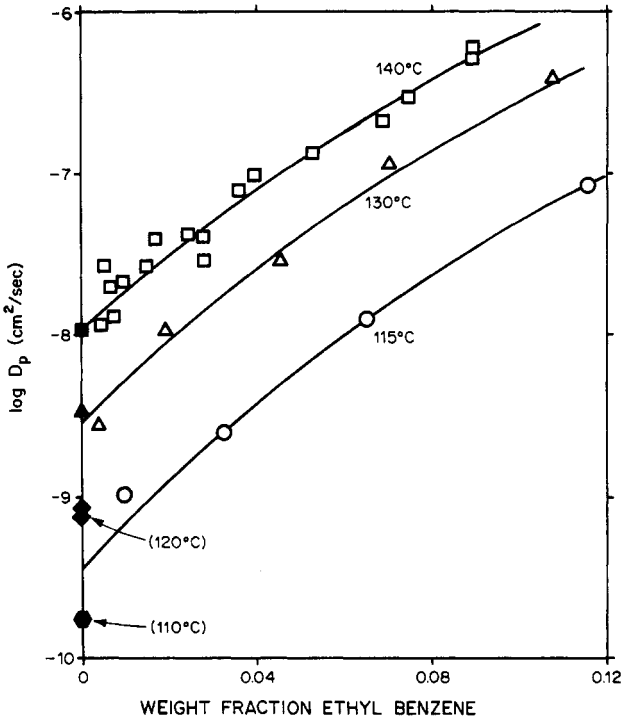

Figure 12. Comparison of IGC and vapor sorption data for the diffusivity of ethylbenzene in polystyrene. Solid symbols indicate infinite dilution diffusivities determined by IGC. The open symbols indicate vapor sorption measurements reported by Duda et al.[43,44]

difference between the techniques would be expected. However, the vapor sorption data reported by Duda et al. give no indication that this is the case. They obtained satisfactory correlations of all their vapor sorption data using temperature and concentration independent interaction parameters.

Diffusion Coefficients. Data regarding the diffusivity of solvents in polymer melts are, in general, very limited; polystyrene is one of the few polymers for which any information is available. The best data available for aromatic solvents are those of Duda, Vrentas, and co-workers. Using a vapor sorption technique, they have obtained an extensive amount of data for the diffusivity of toluene and ethylbenzene in polystyrene.[43,44]

Because vapor sorption studies are virtually always done at finite concentrations, their results cannot be compared directly to the infinite dilution measurements obtained in this study. However, the infinite dilution results of this work can be compared to extrapolations of finite concentration data for a check of consistency. Such a comparison is shown in Figures 11 and 12, which show log D_p vs. weight fraction concentration for toluene and ethylbenzene. The solid symbols on the vertical axis represent average values of the infinite diffusion coefficients measured in this study. The solid lines are extrapolations of the finite concentration data. It is clear from these figures that the data of the present study are highly consistent with previous studies.

As expected, the infinite dilution diffusion coefficient exhibits a strong temperature dependence, with the value changing 2 orders of magnitude over the temperature range studied. Figure 13 shows a plot of log D_p vs. the reciprocal of temperature for the data obtained in this study. For all three solvents, the plots are linear. The apparent energy of activation for the three solvents are 35.3, 41.8, and 44.2 kcal/mol for benzene, toluene, and ethylbenzene. A strong temperature dependence for the diffusivity is common in

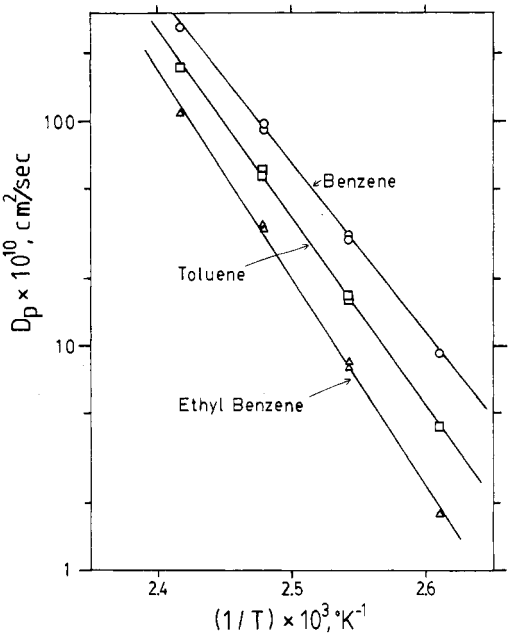

Figure 13. Temperature dependence of the infinite dilution diffusion coefficient.

polymers near their glass transition temperature.[45,48]

Acknowledgment. We thank the National Science Foundation, the Center of the University of Massachusetts/Industry Research on Polymers (CUMIRP), and the University of Massachusetts Computing Center for their support during this research.

Nomenclature

A	constant representing the contributions of eddy diffusion
a_1	activity of the solute in the stationary phase

B	constant representing the contributions of gas-phase molecular diffusion
B_{11}	second virial coefficient
C	constant representing the contributions of mass-transfer resistance
C_i	constant defined by eq 38
c	gas-phase solute concentration
c'	stationary-phase solute concentration
$\mathbf{c}$	mean gas-phase solute concentration
c_0	strength of the inlet impulse
D_e	eddy diffusion coefficient
D_m	solute diffusion coefficient in the mobile phase
D_s	solute diffusion coefficient in the stationary phase
D_g	gas-phase diffusion coefficient for the solute
D_p	solute diffusion coefficient in the stationary phase
F	flow rate of the carrier
H	height equivalent to a theoretical plate (HETP)
K	partition coefficient describing the equilibrium partitioning of solute between phases
L	column length
M_p	mass of the polymer
M_1	molecular weight of the solute
M_2	number-average molecular weight of the polymer
p_1^0	vapor pressure of the solute
q	dimensionless stationary phase concentration, eq 19
$\mathbf{R}$	ideal gas constant
R	radius of the column
r	radial coordinate
S	ratio of the mean sample velocity to the mean carrier gas velocity, V_s/V
T	column temperature
t_c	residence time of the carrier gas
t_m	retention time of the marker
t_r	retention time of the peak
t_s	retention time of the solvent
V_1	molar volume of the solute
V_g^0	specific retention volume
$W_{1/2}$	width of the peak at half-height
w_1	fraction of solute in the stationary phase
V	mean speed of the carrier gas
x	dimensionless axial length, eq 19
y	dimensionless mobile phase concentration, eq 19
z	axial coordinate

Greek Symbols

α	dimensionless partition coefficient, eq 22
β	dimensionless diffusion parameter, eq 22
γ	dimensionless axial dispersion parameter, eq 22
$\delta(t)$	Dirac delta function
Δc	concentration perturbation
ϵ	ratio of the stationary-phase volume to the gas-phase volume
μ_1	first temporal moment or mean residence time
μ_2^*	second central moment or variance of the concentration distribution
μ_k	k-th normalized moment of the elution curve, eq 22
μ_k^*	k-th central moment of the elution curve, eq 33
σ_t^2	variance of the peak
τ	film thickness
η	dimensionless film thickness, eq 19
θ	dimensionless time, eq 19
Ω_1^∞	mass activity coefficient
v_i	specific volume of component i
χ_{12}	Flory–Huggins interaction parameter

Registry No. Polystyrene, 9003-53-6; benzene, 71-43-2; toluene, 108-88-3; ethylbenzene, 100-41-4.

References and Notes

(1) Laub, R. J.; Pecsok, R. L. *Physicochemical Applications of Gas Chromatography*; Wiley: New York, 1978.
(2) Conder, J. R.; Young, C. L. *Physicochemical Applications of Gas Chromatography*; Wiley: New York, 1979.
(3) Braun, J. M.; Guillet, J. E. *Adv. Polym. Sci.* **1976**, *21*, 107.
(4) Gray, D. G. *Prog. Polym. Sci.* **1977**, *5*, 1.
(5) Summers, W. R.; Tewari, Y. B.; Schreiber, H. B. *Macromolecules* **1972**, *5*, 12.
(6) Tewari, Y. B.; Schreiber, H. B. *Macromolecules* **1972**, *5*, 329.
(7) Tait, P. J. T.; Abushihada, A. M. *J. Chromatogr. Sci.* **1979**, *17*, 219.
(8) Vrentas, J. S.; Duda, J. L.; Hsieh, S. T. *Ind. Eng. Chem. Prod. Res. Dev.* **1983**, *22*, 326.
(9) Braun, J. M.; Poos, S.; Guillet, J. E. *Polym. Lett.* **1976**, *14*, 257.
(10) Kong, J. M.; Hawkes, S. J. *Macromolecules* **1975**, *8*, 148.
(11) Millen, W.; Hawkes, S. *J. Chromatogr. Sci.* **1977**, *15*, 148.
(12) Galin, M.; Rupprecht, M. C. *Polymer (Am. Chem. Soc., Div. Polym. Chem.)* **1978**, *19*, 506.
(13) Senich, G. A. *Polym. Prep.*, **1981**, *22*(2), 343.
(14) van Deemter, J. J.; Zuiderweg, F. J.; Klinkenberg, A. *Chem. Eng. Sci.* **1956**, *5*, 271.
(15) Crank, J.; Park, G. S. "Methods of Measurement" In *Diffusion in Polymers*; Crank, J., Park, G. S., Eds.; Academic: New York, 1968.
(16) Crank, J. *The Mathematics of Diffusion*; Clarendon: Oxford, 1975; Chapter 10.
(17) Gray, D. G.; Guillet, J. E. *Macromolecules* **1973**, *6*, 223.
(18) Lichtenthaler, R. N.; Liu, D. D.; Prausnitz, J. M. *Macromolecules* **1974**, *7*, 565.
(19) Macris, A. M.S. Thesis, University of Massachusetts, Amherst, MA, 1979.
(20) Golay, M. J. E. In *Gas Chromatography*; Desty, D. H., Ed.; Butterworths: Washington, D.C., 1958.
(21) Aris, R. *Proc. R. Soc. London* **1959**, *52*, 538.
(22) Khan, M. A. *Gas Chromatography*; van Swaay, M., Ed.; Butterworths: Washington, D.C., 1962.
(23) Taylor, G. I. *Proc. R. Soc. London A* **1953**, *A219*, 186.
(24) Edwards, T. J.; Newman, J. *Macromolecules* **1977**, *10*, 609.
(25) Kubin, M. *Collect. Czech. Chem. Commun.* **1965**, *30*, 1104.
(26) Kucera, E. *J. Chromatogr.* **1965**, *19*, 237.
(27) Douglas, J. M. *Process Dynamics and Control. Analysis of Dynamic Systems*; Prentice-Hall; Englewood Cliffs, NJ, 1972; Vol 1.
(28) Crump, K. S. *J. Assoc. Comput. Mach.* **1976**, *23*, 89.
(29) Ramachandran, P. A.; Smith, J. M. *Ind. Eng. Chem. Fundam.* **1978**, *17*, 148.
(30) Pawlisch, C. A. Ph.D. Dissertation, University of Massachusetts, Amherst, MA, 1985.
(31) Jennings, W. *Gas Chromatography with Glass Capillary Columns*, 2nd ed.; Academic: New York, 1980.
(32) Newman, R. D.; Prausnitz, J. M. *J. Phys. Chem.* **1972**, *76*, 1492.
(33) Patterson, D.; Tewari, Y. B.; Schreiber, H. P.; Guillet, J. E. *Macromolecules* **1971**, *4*, 356.
(34) Billmeyer, F. W. *Textbook of Polymer Science*, 2nd ed.; Wiley: New York, 1971.
(35) Schuster, R. H.; Grater, H.; Cantow, H.-J. *Macromolecules* **1984**, *17*, 619.
(36) Gunduz, S.; Dinçer, S. *Polymer* **1980**, *21*, 1041.
(37) Brockmeier, N. F.; McCoy, R. W.; Meyer, J. A. *Macromolecules* **1972**, *5*, 464.
(38) Covitz, F. H.; King, J. W. *J. Polym. Sci., Part A-1* **1972**, *10*, 689.
(39) Courval, G. J.; Gray, D. G. *Can. J. Chem.* **1976**, *54*, 3496.
(40) Gray, D. G.; Guillet, J. E. *Macromolecules* **1974**, *7*, 244.
(41) Lipatov, Y. S.; Nesterov, A. E. *Macromolecules* **1975**, *8*, 889.
(42) Miltz, J. *Polymer* **1986**, *27*, 105.
(43) Duda, J. L.; Ni, Y. C.; Vrentas, J. S. *J. Appl. Polym. Sci.* **1978**, *22*, 689.
(44) Duda, J. L.; Vrentas, J. S.; Ju, S. T.; Liu, H. T. *AIChE J.* **1982**, *28*, 279.
(45) Vrentas, J. S.; Duda, J. L. *J. Polym. Sci., Polym. Phys. Ed.* **1977**, *15*, 403.
(46) Vrentas, J. S.; Duda, J. L. *J. Polym. Sci., Polym. Phys. Ed.* **1977**, *15*, 417.
(47) Vrentas, J. S.; Duda, J. L. *J. Polym. Sci., Polym. Phys. Ed.* **1977**, *15*, 440.
(48) Vrentas, J. S.; Duda, J. L. *J. Appl. Polym. Sci.* **1977**, *21*, 1715.